Inorganic Chemistry

Article

pubs.acs.org/IC

Photophysical and Photoredox Characteristics of a Novel Tricarbonyl Rhenium(I) Complex Having an Arylborane-Appended Aromatic Diimine Ligand

Akitaka Ito,[†,∥] Yuanyuan Kang,[‡] Shota Saito,[†] Eri Sakuda,[†,‡,§] and Noboru Kitamura*[,†,‡]

[†]Department of Chemistry, Faculty of Science, [‡]Department of Chemical Sciences and Engineering, Graduate School of Chemical Sciences and Engineering, Hokkaido University, Sapporo 060-0810, Japan

[§]PRESTO, Japan Science and Technology Agency (JST), 4-1-8, Honcho, Kawaguchi, Saitama 332-0012, Japan

Supporting Information

ABSTRACT: We report the synthesis and photophysical/photoredox characteristics of a novel tricarbonyl rhenium(I) complex having a (dimesityl)borylduryletheynyl (DBDE) group at the 4-position of a 1,10-phenanthroline (phen) ligand, $[Re(CO)_3(4\text{-DBDE-phen})Br]$ (**ReB**). **ReB** in tetrahydrofuran at 298 K showed the metal-to-ligand charge transfer (MLCT) emission at around 681 nm with the lifetime (τ^{em}) of 900 ns. The relatively long emission lifetime of **ReB** compared with that of $[Re(CO)_3(phen)Br]$ (**RePhen**, τ^{em} = 390 ns) was discussed on the basis of the temperature dependent τ^{em} and Franck−Condon analysis of the emission spectra of the two complexes. Emission quenching studies of both **ReB** and **RePhen** by a series of electron donors revealed that the photoinduced electron transfer (PET) quenching rate constant of **ReB** was faster than that of **RePhen** at a given Gibbs free energy change of the PET reaction ($\Delta G_{ET}^{0} > -0.5$ eV). All of the results on **ReB** were discussed in terms of the contribution of the CT interaction between the π-orbital(s) of the aryl group(s) and the vacant p-orbital on the boron atom in DBDE to the MLCT state of the complex.

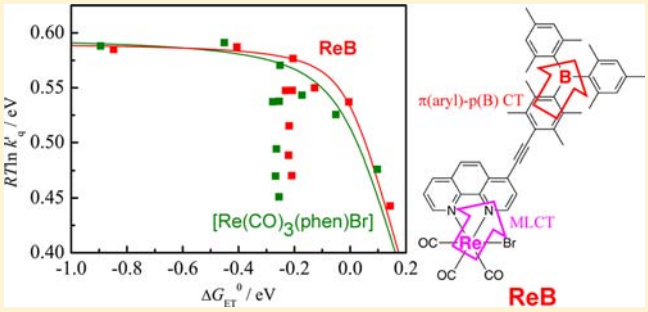

INTRODUCTION

Polypyridine d^6 transition metal complexes are known to show metal-to-ligand charge transfer (MLCT) absorption/phosphorescence, and the design/synthesis of such types of transition metal complexes have received current attention.[1] Among various MLCT-type transition metal complexes, a tricarbonyl rhenium(I) diimine complex, $[Re(CO)_3LX]$ (L = diimine and X = halogen, trialkylphosphine or imine), has been studied extensively owing to its characteristic spectroscopic/photophysical and photoredox properties,[2] including its photocatalytic ability to CO_2 reduction.[3] The spectroscopic, photophysical, and redox properties of $[Re(CO)_3LX]$ are known to be very sensitive to the microenvironments around the complex (i.e., solvent polarity, rigidity of the surrounding phase, and so forth),[2c,k,m,4] compared with those of a polypyridine ruthenium(II) complex, because of the asymmetric structure of $[Re(CO)_3LX]$. Furthermore, these properties of the complex are also sensitive to the nature of L and X.[2a,b,e,f,h,m,r,3e,4b,5] Therefore, chemical modifications and derivatizations of $[Re(CO)_3LX]$ by the nature of L and/or X toward development of efficient photochemical/catalytic reaction systems are of primary importance.

For synthetic modulation of the spectroscopic/photophysical properties of a transition metal complex, we focus on the characteristic electronic structures of a triarylborane, derived from the sp^2-hybridized structure of the boron−carbon bonds and the vacant p-orbital on the boron atom (p(B)) in the electronic ground state.[6] Owing to such electronic structures, a triarylborane compound shows characteristic spectroscopic/photophysical properties ascribed to intramolecular charge transfer (CT) between the π-orbital of the aryl group and p(B) (π(aryl)-p(B) CT),[7] and the π(aryl)-p(B) CT absorption/fluorescence properties of the compound have been reported to be quite sensitive to the nature of the aryl group, the solvent polarity around the molecule,[8] and the molecular packing structures in the crystalline state.[9] The π(aryl)-p(B) CT characters are expected to synergistically interact with the MLCT excited state of a transition metal complex and the metal complex possessing a triarylborane-appended ligand(s) would show new and novel spectroscopic/photophysical properties. In practice, we succeeded in synthetic tuning of the emission quantum yield (Φ^{em}) and lifetime (τ^{em}) of a 2,2′:6′,2″-terpyridine (tpy) platinum(II) complex by introducing a (dimesityl)-phenylborane group at the 4′-position of tpy (Btpy), $[Pt(Btpy)Cl]^+$.[10] $[Pt(Btpy)Cl]^+$ showed relatively intense emission in $CHCl_3$ at room temperature (Φ^{em} = 0.011 and τ^{em} = 0.6 μs) while $[Pt(tpy)Cl]^+$ in solution at room temperature is non-luminescent.[11] We anticipate synergistic MLCT/π(aryl)-p(B)

Received: April 11, 2012
Published: June 28, 2012

   dx.doi.org/10.1021/ic3007469 | Inorg. Chem. 2012, 51, 7722−7732

Scheme 1. Synthetic Routes for ReB: (a) $[Re(CO)_5Br]$, toluene, reflux 2 h, (b) EDDB, $Pd(PPh_3)_2Cl_2$, CuI, NEt_3, THF, 50 °C 2 h

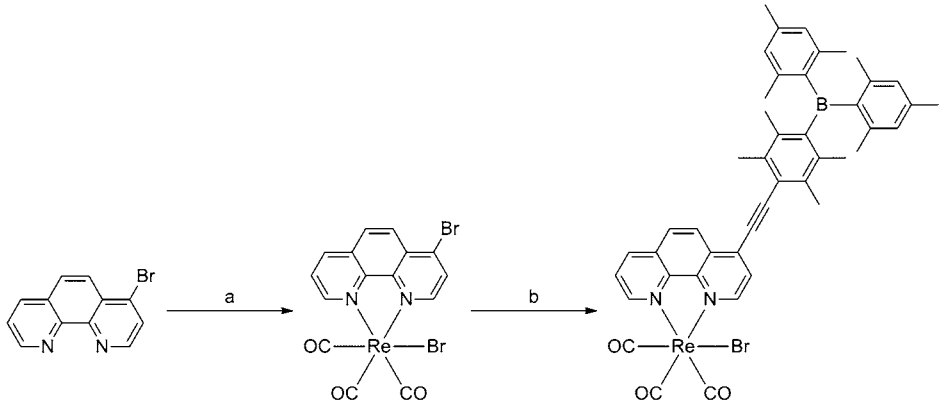

CT interactions can tune the spectroscopic/photophysical properties of various transition metal complexes. After our first report on $[Pt(Btpy)Cl]^+$ in 2006, in practice, a variety of transition metal complexes bearing an arylborane unit(s) on the ligand have been reported: Pt(II),[12] Ir(III),[13] Ru(II),[14] Re(I),[15] Cu(I),[12a,b] and so forth.[16]

Recently, we reported the ruthenium(II) complex bearing a (dimesityl)borylduryllethynyl (DBDE) group at the 4-position of a 1,10-phenanthroline (phen) ligand (**4RuB**$^{2+}$) showed low-energy, extremely long-lived and temperature-independent phosphorescence (maximum wavelength (λ^{em}) = 681 nm and τ^{em} = 12 μs at 298 K in CH_3CN) owing to the stabilization of the emissive triplet MLCT excited state by the synergistic interaction with π(aryl)-p(B) CT and subsequent decrease in the contribution of the nonemitting triplet dd excited state to excited state decay in the MLCT state.[17] Furthermore, we found that the emission from **4RuB**$^{2+}$ was quenched by CO_2 in solution.[18] This is the first experimental observation of direct emission quenching of a transition metal complex by CO_2, and it could be explained by the electrophilic interaction/reaction of CO_2 with the excited electron/charge on the vacant p-orbital on the boron atom in **4RuB**$^{2+}$. These discussions demonstrate that an introduction of an arylborane charge transfer unit to the periphery of the ligand in a transition metal complex affects extraordinary the spectroscopic, photophysical, and photochemical properties of the complex.

In this paper, we report the synthesis, electrochemical, spectroscopic, and photophysical properties of a novel tricarbonyl rhenium(I) complex having a 4-DBDE-phen ligand (**ReB**, see the structure in Scheme 1). Although the diimine ligand employed in the present study is the essentially the same with that reported for **4RuB**$^{2+}$,[17] it is worth studying the generality of the roles of the 4-DBDE-phen ligand in the absorption intensity, Φ^{em}, and τ^{em} in a transition metal complex. Furthermore, we report here emission quenching of **ReB** by a series of aromatic/aliphatic amines and discuss the characteristics of **ReB** as a photoredox sensitizer. Since it has been well recognized that $[Re(CO)_3LX]$ derivatives have high potentials as photosensitizers/photoredox catalysts and the photoredox reaction of $[Re(CO)_3LX]$ with an electron donor is the primary event for photoreduction of CO_2 to CO,[3d,h,j] the photoredox properties of **ReB** are worth studying in detail. In particular, the number of reports on tricarbonyl rhenium(I) diimine complexes having an arylborane charge transfer unit(s) is quite limited.[15] This is the first report on the tricarbonyl rhenium(I) complex having an arylborane-appended aromatic diimine ligand, and we show the important roles of the 4-DBDE-phen ligand in synthetic modulations of the spectroscopic, photophysical, and photoredox properties of a tricarbonyl rhenium(I) diimine complex.

EXPERIMENTAL SECTION

Synthesis of ReB. Scheme 1 shows the synthetic routes for **ReB**. **ReB** was synthesized by utilizing the Sonogashira-Hagiwara cross coupling reaction between (ethynylduryl)dimesitylborane (EDDB) and $[Re(CO)_3(4\text{-Br-phen})Br]$, similar to the procedures for synthesizing **4RuB**$^{2+}$.[17] EDDB was synthesized according to the literature with some modifications, as reported in the Supporting Information.[19]

All of the chemicals used for the synthesis of **ReB** were purchased from Wako Pure Chemical Ind., Kanto Chemical Co. Inc., Tokyo Kasei Kogyo Co. Ltd., or Sigma-Aldrich Co. and used as supplied. Column chromatography was carried out by using Merck aluminum oxide 90 standardized or GE Healthcare Sephadex LH-20.

^{1}H NMR spectra were recorded on a JEOL JME-EX270 FT-NMR system (270 MHz). The chemical shifts of the spectra determined in $CDCl_3$ were given in ppm with tetramethylsilane being an internal standard (0.00 ppm). Electrospray ionization (ESI) mass spectra were recorded on a Waters micromass ZQ spectrometer.

Synthesis of fac-Bromotricarbonyl(4-bromo-1,10-phenanthroline)rhenium(I) ([Re(CO)$_3$(4-Br-phen)Br]). Bromopentacarbonylrhenium(I) ($[Re(CO)_5Br]$, 0.4965 g, 1.22 mmol) and 4-bromo-1,10-phenanthroline (4-Br-phen, 0.3110 g, 1.20 mmol)[17,20] were stirred in toluene (50 mL) until the reactants were completely dissolved. After refluxing the mixture for 2 h under Ar gas atmosphere, the solvent was removed under reduced pressure. The crude product was purified by column chromatography (Al_2O_3, chloroform), afforded the facial isomer of $[Re(CO)_3(4\text{-Br-phen})Br]$ as an orange powder with a high purity for the following reaction (>90%, 0.69 g, 84%). R_f = 0.42 (Al_2O_3, chloroform). ^{1}H NMR (270 MHz, $CDCl_3$): δ 7.92 (ddd, 1H, J = 0.43, 5.2, 8.3 Hz, 8-Ar-H), 8.14 (d, 1H, J = 4.8 Hz, 3−Ar−H), 8.13 (d, 1H, J = 5.5 Hz, 6−Ar−H), 8.38 (dd, 1H, J = 4.2, 4.7 Hz, 5−Ar−H), 8.60 (dd, 1H, J = 0.84, 8.3 Hz, 7−Ar−H), 9.18 (d, 1H, J = 5.6 Hz, 2−Ar−H), 9.46 (dd, 1H, J = 0.92, 5.2 Hz, 9−Ar−H). ESI-MS m/z 529 ($[M-Br]^+$).

*Synthesis of fac-Bromotricarbonyl[4-(dimesitylboryl)-durylethynyl-1,10-phenanthroline]rhenium(I) (**ReB**).* After an oven-dried Schlenk tube was evacuated and filled with an Ar gas, $[Re(CO)_3(4\text{-Br-phen})Br]$ (464 mg, 0.76 mmol), CuI (17.9 mg, 0.094 mmol), and $Pd(PPh_3)_2Cl_2$ (32 mg, 0.046 mmol) were added. An argon gas-purged tetrahydrofuran (THF)/triethylamine (22 mL/10 mL) mixture was added to the tube and stirred for 15 min at room temperature. A THF (16 mL) solution of EDDB (410 mg, 1.0 mmol) was then added dropwise to the reaction mixture. The mixture was stirred at 50 °C for 2 h under N_2 gas atmosphere and, then, cooled to room temperature. The

dx.doi.org/10.1021/ic3007469 | Inorg. Chem. 2012, 51, 7722−7732

insoluble solids were removed by filtration through Celite and washed with a large amount of toluene. The crude product was purified by column chromatography (LH-20, ethanol/chloroform =1/2, v/v) and successive recrystallizations from toluene. Binary phase diffusion of the toluene solution of the crude product to cyclohexane afforded the facial-isomer of **ReB** as a dark orange powder (0.11 g, 15%). R_f = 0.42 (Al_2O_3, chloroform). ^{1}H NMR (270 MHz, $CDCl_3$): δ 1.99 (s, 12 H, *ortho*-CH_3 of mesityl), 2.08 (s, 6 H, *ortho*-CH_3 of duryl), 2.28 (s, 6H, *para*-CH_3 of mesityl), 2.54 (s, 6H, *meta*-CH_3 of duryl), 6.77 (s, 4H, Ar−H of mesityl), 7.89 (dd, 1H, J = 5.0, 8.2 Hz, 8−Ar−H of phen), 7.92 (d, 1H, J = 5.5 Hz, 3−Ar−H of phen), 8.08 (d, 1H, J = 9.0 Hz, 6−Ar−H of phen), 8.56 (dd, 1H, J = 1.8, 8.4 Hz, 7−Ar−H of phen), 8.56 (d, 1H, J = 8.9 Hz, 5−Ar−H of phen), 9.33 (d, 1H, J = 5.5 Hz, 2−Ar−H of phen), 9.43 (dd, 1H, J = 1.4, 5.2 Hz, 9−Ar−H of phen). ESI-MS m/z 856 ([M−Br]$^+$). Anal. calcd. for $C_{45}H_{41}BBrN_2O_3Re{\cdot}0.1CHCl_3$: C, 57.22; H, 4.38; N, 2.96; X (Br + Cl), 9.56. Found: C, 56.95; H, 4.42; N, 3.09; X, 9.28.

Other Chemicals. Spectroscopic grade THF and toluene (Dojindo Molecular Technologies, Inc.) were used as supplied. Other solvents for spectroscopic and electrochemical measurements were distilled prior to use.[21] Organic quenchers used in the present study were purified by the accepted procedures. *fac*-Bromotricarbonyl(1,10-phenanthroline)-rhenium(I) (**RePhen**) as a reference complex for **ReB** was synthesized according to the reported procedures,[2f] and its structure was confirmed by ^{1}H NMR spectroscopy and mass spectrometry. ^{1}H NMR (270 MHz, $CDCl_3$): δ 7.91 (dd, 1H, J = 5.1, 8.3 Hz, 3−Ar−H), 8.06 (s, 1H, 5−Ar−H), 8.58 (dd, 1H, J = 1.4, 8.3 Hz, 4−Ar−H), 9.45 (dd, 1H, J = 1.4, 5.0 Hz, 2−Ar−H). ESI-MS m/z 451 ([M−Br]$^+$).

Spectroscopic and Electrochemical Measurements. Absorption and corrected emission spectra of **ReB** and **RePhen** were measured by using a Hitachi UV-3300 spectrophotometer and a Hamamatsu multichannel photodetector (PMA-11, excitation wavelength = 355 nm), respectively. The absolute emission quantum yields of the complexes were measured by a Hamamatsu C9920-02 system equipped with an integrating sphere and a red-sensitive multichannel photodetector (PMA-12, excitation wavelength = 400 nm).[22] The absorbance of a sample solution was set <0.05 at the excitation wavelength. Emission lifetime measurements were conducted by using a streak camera (Hamamatsu Photonics, C4334) as a photodetector at 355-nm laser pulse excitation (LOTIS TII Ltd., LS-2137). A liquid N_2 cryostat (DN1704 optical Dewar and 3120 temperature controller, Oxford Instruments) was used to control a sample temperature. For emission spectroscopy, sample solutions were deaerated by purging an argon-gas stream over 30 min.

Cyclic and differential pulse voltammetries were conducted by using an electrochemical analyzer (BAS, ALS-701A) with a three-electrodes system using Pt working, Pt auxiliary, and SCE reference electrodes. The concentrations of the complexes or quenchers in *N*,*N*-dimethylformamide (DMF) were set at 1×10^{-3} mol/dm^3 (M), and 0.10 M of tetra-*n*-butylammonium hexafluorophosphate ($TBAPF_6$) was used as a supporting electrolyte. Sample solutions were deaerated by purging an Ar-gas stream over 20 min prior to the experiments. The potential sweep rate was set to 100 mV/s in cyclic voltammetry and differential pulse voltammetry was conducted with 50 mV height pulses (0.05 s duration) being stepped by 5.0 mV intervals (2.0 s interval between the two pulses).

Theoretical Calculations. The calculations on the electron densities of **ReB** and **RePhen** were conducted on the Gaussian 09W programs.[23] Optimizations of the structures of the complexes in the ground state were performed by using the B3LYP density functional theory (DFT). The LANL2DZ and 6-31G(d,p) basis sets were used to treat the rhenium atom and all other atoms, respectively. Time-dependent DFT (TD-DFT) calculations were then performed to estimate the energies and oscillator strengths of the ten lowest-energy transitions of the complexes. The contours of the electron density were plotted by using GaussView 5.0.

Franck−Condon Analysis of the Emission Spectra at Room Temperature. Franck−Condon analysis is a spectral fitting analysis which provides information about the electronic and vibrational structures of an excited-state molecule, and the fundamental equation is given in eq 1.[24]

$$I(\tilde{\nu}) = \sum_{\nu_M=0}^{\infty}\sum_{\nu_L=0}^{\infty}\left(\frac{E_0 - \nu_M\hbar\omega_M - \nu_L\hbar\omega_L}{E_0}\right)^4\left(\frac{S_M{}^{\nu_M}}{\nu_M!}\right)\left(\frac{S_L{}^{\nu_L}}{\nu_L!}\right)$$
$$\exp\left[-4\ln 2\left(\frac{\tilde{\nu} - E_0 + \nu_M\hbar\omega_M + \nu_L\hbar\omega_M}{\tilde{\nu}_{1/2}}\right)^2\right] \quad (1)$$

In eq 1, $I(\tilde{\nu})$ is the emission intensity at the energy in wavenumber (cm^{-1}) relative to that of the 0→0 transition. E_0 is the energy gap between the zeroth vibrational levels in the ground and excited states. $\hbar\omega_M$ and $\hbar\omega_L$ are the quantum spacings for averaged medium- and low-frequency vibrational modes governing nonradiative decay of a molecule, respectively. S_M and S_L are the Huang−Rhys factors[25] reflecting nuclear distortions along the coordinates of the medium- and low-frequency quantum modes, respectively. $\tilde{\nu}_{1/2}$ is the full width at half-maximum (fwhm) for an individual vibronic line. The photon numbers of the emission spectrum were corrected in a wavenumber scale by using the equation $I(\tilde{\nu}) = I(\lambda) \times \lambda^2$,[26] and the parameters E_0, S_M, S_L, $\hbar\omega_M$, $\hbar\omega_L$, and $\tilde{\nu}_{1/2}$ were optimized with a least-squares minimization routine using a Generalized Reduced Gradient (GRG2) algorithm.[27] The summation was carried out over 11 vibrational levels for both ν_M and ν_L: 0 → 10.

Determination of the Quenching Rate Constant (k_q) and the Free Energy Change of the Photoinduced Electron Transfer (PET) Process ($\Delta G_{ET}{}^0$). Scheme 2 shows the kinetic scheme of PET quenching of the excited state of [Re(CO)$_3$LX] (Re^I*) by an electron donor (D). In this scheme, k_d and k_{-d} represent the association and dissociation rate constants of the reactants and the encounter complex (Re^I*·····D), respectively. k_{ET} is the forward ET rate constant in the encounter complex, and k_{-ET} is the backward ET rate constant in the ion pair (Re^0·····D^+) giving the encounter complex. k_{BET} and k''_{-d} are the rate constants of the backward ET reaction giving the ground state complex (Re^I·····D) and subsequent dissociation of the ground state complex, respectively. k'_{-d} is the rate constant of the free ion formation process, and k'_d is the association rate constant of the free ions producing the ion pair. The emission quenching rate constant (k_q) of **ReB** or **RePhen** by a given D as a quencher was determined by the Stern−Volmer equation in eq 2,

Scheme 2. Kinetic Scheme for PET Quenching of a Tricarbonyl Rhenium(I) Diimine Complex (Re^I) by an Electron Donor (D)

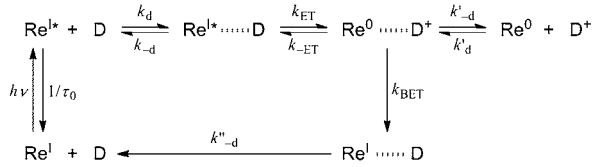

$$\frac{\tau_0}{\tau} = 1 + k_q\tau_0[D] \quad (2)$$

where τ_0 and τ are the emission lifetimes of **ReB** or **RePhen** in the absence and presence of D, respectively, and [D] is the quencher concentration. Since the observed k_q includes the contributions from both k_{ET} and k_d, the latter contribution to the observed k_q value has been corrected by eq 3.

$$k'_q{}^{-1} = k_q{}^{-1} - k_d{}^{-1} \quad (3)$$

In eq 3, the k_d value has been estimated by the Smoluchowski equation, eq 4,[28]

$$k_d = \frac{2RT}{3000\eta}\left(2 + \frac{r_D}{r_A} + \frac{r_A}{r_D}\right) \quad (4)$$

where R, T, and η are the gas constant, temperature, and the viscosity of a medium, respectively. The radii of the complex and a quencher (r_A and r_D, respectively) were evaluated based on the optimized ground-state

dx.doi.org/10.1021/ic3007469 | Inorg. Chem. 2012, 51, 7722−7732

structure of each complex or D by DFT calculations. The r_A values of **ReB** and **RePhen** were 7.2 and 5.3 Å, respectively, and the r_D values are shown in a later section.

The Gibbs free energy change for the PET reaction (ΔG_{ET}^0) of **ReB** or **RePhen** by D has been calculated based on eq 5,[1b,29]

$$\Delta G_{ET}^{\ 0} = E_{1/2}(D^{+/0}) - E_{1/2}(Re^{+/0}) - E_0 + w_p - w_r \quad (5)$$

where $E_{1/2}(Re^{+/0})$ and $E_{1/2}(D^{+/0})$ are the reduction and oxidation potentials of **ReB** or **RePhen** and D, respectively, and E_0 is the excited-state energy of the complex. The E_0 values of **ReB** and **RePhen** in DMF were determined to be 15850 and 18180 cm^{-1}, respectively, by the Franck−Condon analysis of the room temperature emission spectra of the complexes: see also Supporting Information (Figure S1 and Table S1). In eq 5, w_p and w_r are the electrostatic works necessary to bring together the two product ions and the reactants from an infinite distance to the close-contact distance for PET, $d = (r_A + r_D)$, respectively. In the present case, $w_r = 0$ since the metal complex and all quenchers used possess no electrical charge. The w_p value was calculated by eq 6,

$$w_p = \frac{Z_{D+}Z_{A-}e^2}{D_s d} \quad (6)$$

where Z_{D+} and Z_{A-} are the charges of the two product ions and, e and D_s are the elementary electric charge and the static dielectric constant of a medium, respectively.

RESULTS AND DISCUSSION

Absorption Spectra. Figure 1 shows the absorption spectra of **ReB** in toluene, THF, and CH_3CN, together with those of

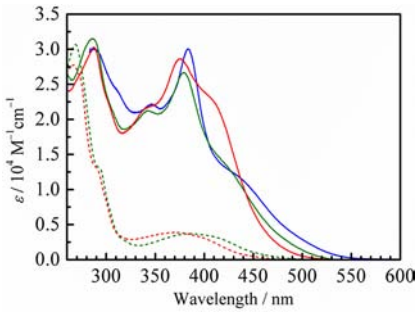

Figure 1. Absorption spectra of **ReB** (solid curves) and **RePhen** (broken curves) in toluene (blue), THF (green), and CH_3CN (red).

RePhen as a reference, and Table 1 summarizes the spectroscopic data of the complexes. **ReB** exhibited the absorption bands at around λ^{abs} (wavelength) = 287 and 380 nm, irrespective of the solvent. The absorption band at around 287 nm could be ascribed to the $\pi\pi^*$ transition of the ligand (ligand-centered (LC) transition) due to the close similarity of the molar absorption coefficient (ε) to that of **RePhen** (ε_{287} = 3.15×10^4 M^{-1} cm^{-1} for **ReB** and $\varepsilon_{269} = 3.07 \times 10^4$ M^{-1} cm^{-1} for **RePhen** in THF). The maximum energy of the LC band observed for **ReB** (λ^{abs} = 287 nm, ν^{abs} (wavenumber) = 34 800 cm^{-1}) was lowered by ∼2400 cm^{-1} compared with that of **RePhen** (λ^{abs} = 269 nm, ν^{abs} = 37 200 cm^{-1}). This could be due to the stabilization of the lowest-energy unoccupied molecular orbital (LUMO) of the phen ligand through an introduction of the arylborane substituent. The ε value of **ReB** at 380 nm (2.67×10^4 $M^{-1}cm^{-1}$ in THF) was almost 7 times larger than that of the MLCT absorption band of **RePhen** ($\varepsilon_{385} = 0.37 \times 10^4$ $M^{-1}cm^{-1}$ in THF), although the maximum energies of the complexes were almost comparable with each other: ν^{abs} = 26 300 and 26 000 cm^{-1} for **ReB** and **RePhen**, respectively. We assigned the band observed for **ReB** at around 380 nm to the superposition of the π(aryl)-p(B) CT and d(Re(I))-to-π^*(durylethynyl-phen) CT transitions owing to the close similarities of the spectral band shape and the ε value to those observed for the ruthenium(II) complex having the same DBDE-substituted ligand with that of **ReB** (i.e., **4RuB**$^{2+}$) in 350−390 nm.[17] The MLCT absorption band of **ReB** was also observed as a shoulder at around 420 nm. A bathochromic shift and an increase in the ε value (λ^{abs} = 420 nm, $\varepsilon_{420} = 1.39 \times 10^4$ $M^{-1}cm^{-1}$) compared with the relevant value of **RePhen** (λ^{abs} = 385 nm, $\varepsilon_{385} = 0.37 \times 10^4$ $M^{-1}cm^{-1}$) can be explained by the electron-accepting ability of the DBDE group in **ReB**, similar to those observed for **4RuB**$^{2+}$.[17] The MLCT absorption band of **ReB** showed a hypsochromic shift with an increase in a solvent polarity ($\Delta\nu \sim 1500$ cm^{-1}). Since the similar absorption spectral shift with a variation of a solvent polarity was also observed for **RePhen** ($\Delta\nu \sim 1520$ cm^{-1}), the results of both complexes will be explained by the stabilization of the ground state of the complex by a solvent polarity.

Cyclic and Differential Pulse Voltammograms. The DBDE group at the 4-position on the phen ligand acts as an electron-accepting unit owing to the presence of p(B), and this should reflect on the redox potentials of **ReB**. Figure 2 shows the

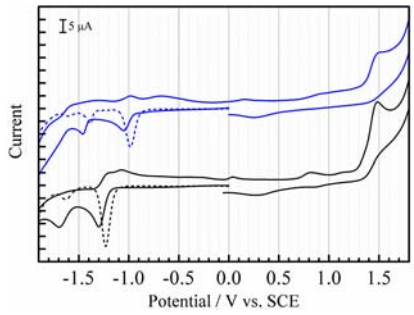

Figure 2. Cyclic voltammograms (solid curves) of **ReB** (blue) and **RePhen** (black) in DMF in the presence of 0.10 M $TBAPF_6$. Broken curves correspond to the differential pulse voltammograms of the complexes. Scan rate = 100 mV/s.

Table 1. Spectroscopic and Photophysical Properties of ReB and RePhen

complex	solvent	λ^{abs}, nm (ε, 10^4 $M^{-1}cm^{-1}$)			λ^{em}, nm	Φ^{em}	τ^{em}, ns	k_r, 10^5 s^{-1}	k_{nr}, 10^5 s^{-1}
ReB	toluene	288 (3.00)	384 (3.00)	438 (sh, 1.15)	669	0.033	1570	0.21	6.1
	THF	287 (3.15)	380 (2.67)	420 (sh, 1.39)	681	0.017	900	0.19	11
	CH_3CN	287 (3.02)	375 (2.86)	411 (sh, 2.23)	676	0.015	960	0.16	10
RePhen	toluene	n.d. (n.d.)[a]		392 (n.d.)[a]	605	0.070	560	1.3	17
	THF	269 (3.07)		385 (0.37)	613	0.044	390	1.1	24
	CH_3CN	267 (2.78)		370 (0.39)	611	0.043	370	1.2	26

[a]Not determined owing to low solubility of the complex.

dx.doi.org/10.1021/ic3007469 | Inorg. Chem. 2012, 51, 7722−7732

cyclic and differential pulse voltammograms of **ReB** and **RePhen** in DMF, and Table 2 summarizes the redox potentials of the

Table 2. Redox Potentials of ReB and RePhen in DMF (0.1 M $TBAPF_6$)[a]

	potential, V (vs SCE)			
complex	$E^{red(3)}$	$E^{red(2)}$	$E^{red(1)}$	E^{ox}
ReB	−1.61	−1.38	−0.98	+1.45
RePhen		−1.63	−1.23	+1.42

[a] [**ReB**] = 1.03 × 10^{-3} M, [**RePhen**] = 0.99 × 10^{-3} M.

complexes. As seen in Figure 2, **RePhen** showed the metal oxidation wave ($E^{ox} = E_{1/2}(Re^{2+/+})$) at +1.42 V (vs SCE) and the peaks responsible for the reduction of phen ($E^{red(1)} = E_{1/2}(Re^{+/0})$) and dissociative reduction of the bromine ligand ($E^{red(2)}$) at −1.23 and −1.63 V, respectively. **ReB** also exhibited E^{ox}, $E^{red(1)}$, and $E^{red(2)}$ at +1.45, −0.98, and −1.38 V, respectively. The E^{ox} value of **ReB** was almost comparable with that of **RePhen**, while both $E^{red(1)}$ and $E^{red(2)}$ were shifted to the positive side by ∼250 mV compared with the relevant value of **RePhen**. These results can be explained by the increase in the electron-accepting ability of **ReB** by the presence of the DBDE group in the phen ligand and, thus, the presence of p(B). In particular, it is worth pointing out that the positive shift of $E^{red(1)}$ by ∼250 mV (∼2000 cm^{-1}) observed for **ReB** compared with that of **RePhen** agrees very well with the difference in ν^{abs} between the two complexes (∼2200 cm^{-1}). These discussions demonstrate clearly that the presence of p(B) on the phen ligand in **ReB** influences strongly the electronic structures of both ground and excited states of the complex. In addition to the positive potential shifts of $E^{red(1)}$ and $E^{red(2)}$ observed for **ReB** relative to those of **RePhen**, furthermore, **ReB** showed the third reduction wave ($E^{red(3)}$) at −1.61 V ascribed to the reduction of the boron atom in the DBDE group. This could play important roles in the physicochemical properties of **ReB**, not expected for those of **RePhen**, as discussed in the following sections.

Time-Dependent Density Functional Theory (TD-DFT) Calculations. To confirm the above discussions, we conducted TD-DFT calculations as the electron density maps in the highest-energy occupied molecular orbital (HOMO) and lowest-energy unoccupied MO (LUMO) levels in **ReB** and **RePhen** were shown in Figure 3. The contributions of the electron densities in the eight components to those in several HOMOs/LUMOs and the details of the 10 lowest-energy absorption transitions estimated by the calculations are also summarized in Tables 3 and 4, respectively.

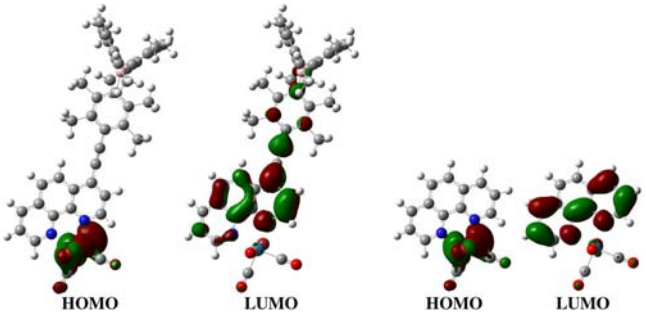

Figure 3. HOMO and LUMO representations of **ReB** and **RePhen** evaluated by DFT calculations.

According to our calculations, the lowest-energy absorption transitions in **ReB** and **RePhen** are ascribed to the HOMO → LUMO (83%)/LUMO+1 (17%) transition at 648 nm with the oscillator strength of f = 0.005 and HOMO → LUMO at 608 nm with f = 0.001, respectively. The HOMOs of both **ReB** and **RePhen** are characterized by the electron densities on the Re(I) and Br atoms. The excited electron in the LUMO of **ReB** distributes from the Re(I) atom to p(B) through the phen and durylethynyl groups of the complex as summarized in Table 3, while that of **RePhen** is localized primarily on the phen ligand. The results support clearly our assignment of the lowest-energy absorption band of **ReB** to the synergistic MLCT/π(aryl)-p(B) CT. Furthermore, the calculated f values of the 10 lowest transitions in **ReB** (e.g., f = 0.900 at the sixth excitation transition, 423 nm) were quite large compared with those in **RePhen** (f ∼ 0.046 at eighth and nineth excitation transitions, 377 and 361 nm, respectively) as seen in Table 4. The results also support the large molar absorption coefficient observed for **ReB**: ε_{420} = 1.39 × 10^4 M^{-1} cm^{-1} in THF.

Emission Spectra and Photophysical Properties at Room Temperature. Figure 4 shows the emission spectra of **ReB** and **RePhen** in toluene, THF, and CH_3CN at 298 K, where the emission intensities of the complexes are normalized to those at the maximum wavelengths (λ^{em}). The emission data are included in Table 1, together with the Φ^{em} and τ^{em} values of the complexes. The emission spectrum of **ReB** (λ^{em} = 669, 681, or 676 nm in toluene, THF, or CH_3CN, respectively) was red-shifted compared with the relevant value of **RePhen** (λ^{em} = 605, 613, or 611 nm, respectively), and the energy difference in the emission maximum ($\Delta\nu^{em}$) between the two complexes in a given solvent was ∼1600 cm^{-1}. The emission from **ReB** is best characterized by the synergistic MLCT/π(aryl)-p(B) CT transition, and the red-shifted emission relative to that from **RePhen** could be explained by the stabilization of the excited state of **ReB** by the presence of the DBDE group at the 4-position of the phen ligand, which is supported by the absorption spectrum, the redox potential, and the TD-DFT calculation, as described above.

Although **ReB** exhibited the red-shifted emission compared with **RePhen**, the emission lifetime of **ReB** (τ^{em} = 900 ns in THF) was longer than that of **RePhen** (τ^{em} = 390 ns), while the emission quantum yield of **ReB** (Φ^{em} = 0.017 in THF) was lower slightly than that of **RePhen** (Φ^{em} = 0.044). The τ^{em} and Φ^{em} values of the complexes in THF give rise to the radiative (k_r) and nonradiative decay rate constants (k_{nr}) to be k_r = 0.19 × 10^5 and k_{nr} = 1.1 × 10^6 s^{-1} for **ReB** and k_r = 1.1 × 10^5 and k_{nr} = 2.4 × 10^6 s^{-1} for **RePhen**, as evaluated by the relations $\Phi^{em} = k_r/(k_r + k_{nr})$ and $\tau^{em} = 1/(k_r + k_{nr})$, see Table 1. These values indicate that the k_r and k_{nr} values of **ReB** are 5.8 and 2.2 times smaller, respectively, than the relevant value of **RePhen**. The results demonstrate that the presence of the DBDE group on the phen ligand in **ReB** influences largely the photophysical parameters of the complex (i.e., τ^{em}, Φ^{em}, k_r, and k_{nr}), which should be discussed in some more detail to reveal the characteristics of the transition metal complex having an arylborane-appended ligand.

Generally, the decrease in the energy gap between the excited and ground states and, thus, a lower-energy shift of ν^{em} results in fast nonradiative decay from the excited state owing to the increase in the electronic coupling between the two states: energy gap dependence of k_{nr}, $\ln k_{nr} \propto \nu^{em}$.[1c,5a,24a,30] Nonetheless, the k_{nr} value of **ReB** was smaller than that of **RePhen**, while **ReB** showed lower-energy emission than **RePhen**. These results cannot be obviously explained by the energy gap dependence of

dx.doi.org/10.1021/ic3007469 | Inorg. Chem. 2012, 51, 7722−7732

Table 3. Electron Density Populations of ReB and RePhen

		contribution, %							
			diimine						
complex	molecular orbital	rhenium	phen	ethynyl	duryl	boron	mesityl	CO	bromide
ReB	206 (LUMO+3)	0.56	74.09	5.83	9.70	1.62	7.48	0.42	0.29
	205 (LUMO+2)	0.06	8.80	1.21	17.06	27.81	44.95	0.07	0.04
	204 (LUMO+1)	1.86	94.00	0.20	0.57	0.06	0.07	2.06	1.14
	203 (LUMO)	2.53	69.69	9.77	10.85	1.38	1.90	2.49	1.38
	202 (HOMO)	27.29	2.74	0.18	0.19	0.00	0.02	14.21	55.36
	201 (HOMO−1)	24.96	4.88	0.59	0.32	0.01	0.03	11.23	57.97
	200 (HOMO−2)	6.93	18.88	14.35	31.53	0.54	6.47	4.10	17.20
	199 (HOMO−3)	67.83	3.03	0.17	0.20	0.00	0.05	28.43	0.30
RePhen	97 (LUMO+3)	9.29	71.82					17.74	1.01
	96 (LUMO+2)	1.83	95.13					1.80	1.25
	95 (LUMO+1)	0.20	99.24					0.55	0.01
	94 (LUMO)	3.92	89.76					3.85	2.47
	93 (HOMO)	27.14	2.62					14.15	56.10
	92 (HOMO−1)	24.68	4.93					11.01	59.37
	91 (HOMO−2)	68.26	2.96					28.46	0.32
	90 (HOMO−3)	34.15	14.43					15.08	36.35

Table 4. Calculated Energy Levels for ReB and RePhen

	ReB			RePhen		
excited state	transition	energy (wavelength)	oscillator strength	transition	energy (wavelength)	oscillator strength
1	HOMO → LUMO (83%) HOMO → LUMO+1 (17%)	1.9134 eV (647.98 nm)	0.0050	HOMO → LUMO	2.0376 eV (608.49 nm)	0.0006
2	HOMO−1 → LUMO (80%) HOMO → LUMO (20%)	2.0036 eV (618.81 nm)	0.0575	HOMO−1 → LUMO	2.1463 eV (577.68 nm)	0.0179
3	HOMO → LUMO+1	2.2007 eV (563.39 nm)	0.0048	HOMO−1 → LUMO (19%) HOMO → LUMO+1 (81%)	2.2463 eV (551.95 nm)	0.0074
4	HOMO−1 → LUMO+1	2.2692 eV (546.37 nm)	0.0112	HOMO−1 → LUMO+1	2.2875 eV (542.01 nm)	0.0041
5	HOMO−3 → LUMO (80%) HOMO−3 → LUMO+1 (20%)	2.7648 eV (448.44 nm)	0.0008	HOMO−2 → LUMO	2.8829 eV (430.06 nm)	0.0001
6	HOMO−2 → LUMO	2.9303 eV (423.11 nm)	0.9002	HOMO−2 → LUMO+1	3.1061 eV (399.17 nm)	0.0000
7	HOMO−3 → LUMO+1	3.0626 eV (404.83 nm)	0.0003	HOMO−4 → LUMO (78%) HOMO−3 → LUMO (22%)	3.1956 eV (387.98 nm)	0.0006
8	HOMO−6 → LUMO (86%) HOMO−6 → LUMO+1 (14%)	3.0690 eV (403.98 nm)	0.0152	HOMO−3 → LUMO	3.2847 eV (377.46 nm)	0.0458
9	HOMO → LUMO+2 (84%) HOMO → LUMO+3 (16%)	3.1271 eV (396.48 nm)	0.0026	HOMO−4 → LUMO+1 (42%) HOMO−3 → LUMO (21%) HOMO−3 → LUMO+1 (24%) HOMO−1 → LUMO+2 (13%)	3.4350 eV (360.94 nm)	0.0463
10	HOMO−2 → LUMO+1	3.1467 eV (394.01 nm)	0.0594	HOMO−3 → LUMO+1 (71%) HOMO → LUMO+2 (29%)	3.4383 eV (360.60 nm)	0.0152

k_{nr}. It has been known that another factor governing k_{nr} of a transition metal complex is thermal activation from the emissive MLCT excited state to the nonemitting dd (ligand-field)/higher-energy lying (fourth) MLCT excited states and subsequent fast nonradiative decay to the ground state.[31] If such thermal processes participate in excited-state decay, the emission lifetime of the complex should depend strongly on temperature (T), which is worth studying in some more detail.

Temperature Dependence of the Emission Lifetime. T-dependences of the emission decay profiles of **ReB** and **RePhen** in propylene carbonate were measured in the range 220−330 K, as shown in Figure S2, Supporting Information. For both complexes, the emission decay profiles were fitted by single exponential functions irrespective of T and the emission lifetimes decreased upon T elevation from 220 to 330 K, as shown in Figure 5: 800−1460 ns for **ReB** and 300−600 ns for **RePhen**. The T dependent emission of a tricarbonyl rheium(I) diimine complex has been sometimes discussed in terms of the contribution of fast nonradiative decay through a higher-energy lying nonemitting fourth MLCT excited state. In such a case, the T dependent emission lifetime of the complex can be analyzed by the following equation, eq 7:[2d]

$$(\tau^{em})^{-1} = \frac{(k_r + k_{nr1}) + k_{nr2}\exp(-\Delta E/RT)}{1 + \exp(-\Delta E/RT)} \quad (7)$$

where k_r and k_{nr1} are the T-independent radiative and nonradiative decay rate constants from the emitting ^{3}MLCT excited state to the ground state, respectively, and k_{nr2} is the nonradiative decay rate constant from the higher-energy nonemitting excited state through thermal activation from the

dx.doi.org/10.1021/ic3007469 | Inorg. Chem. 2012, 51, 7722−7732

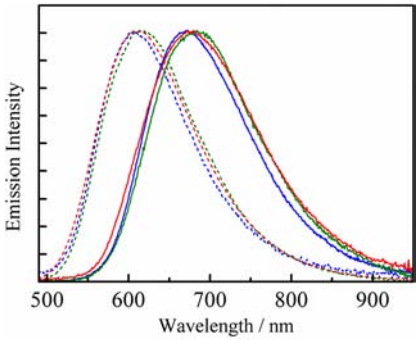

Figure 4. Corrected emission spectra of **ReB** (solid curves) and **RePhen** (broken curves) in toluene (blue), THF (green), and CH_3CN (red) at 298 K.

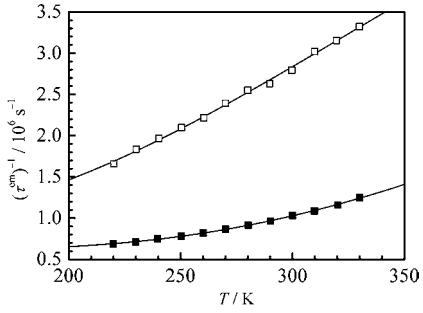

Figure 5. Temperature dependences of the emission lifetimes of **ReB** (closed boxes) and **RePhen** (open boxes) in propylene carbonate. Solid curves represent the theoretical fits based on eq 7.

^{3}MLCT state to the state with the energy barrier being ΔE. The electronic distribution between the two states is corrected by the denominator in eq 7 due to their small energy difference. The T dependent τ^{em} data of **ReB** and **RePhen** were then simulated by eq 7 as the results were shown by the black curves in Figure 5. The data were adequately fitted by eq 7, and the ΔE values of **ReB** and **RePhen** were determined to be 960 and 560 cm^{-1}, respectively, as summarized in Table 5. The ΔE value of **ReB** is

Table 5. *T*-Dependent Emission Parameters for ReB and RePhen in Propylene Carbonate

complex	$(k_r + k_{nr1})$, s^{-1}	k_{nr2}, s^{-1}	ΔE, cm^{-1}
ReB	6.1×10^5	4.3×10^7	960
RePhen	9.4×10^5	3.0×10^7	560

1.7-times larger than that of **RePhen**, and the results strongly suggest that the increase in τ^{em} observed for **ReB** will be explained by the decrease in the contribution of thermal activation to the higher-energy nonemitting excited state to excited decay of the emitting ^{3}MLCT state.

Franck–Condon Analysis of the Emission Spectrum at Room Temperature. To discuss further the effects of the DBDE group on nonradiative decay of **ReB**, we conducted Franck–Condon analysis of the emission spectrum of **ReB**. Figure 6 shows the corrected and simulated emission spectra (i.e., simulated by eq 1) of **ReB** in THF at 298 K together with those of **RePhen**, and the optimized spectral fitting parameters are summarized in Table 6. Both spectra were reproduced almost satisfactorily by assuming the two accepting vibrational modes of $\hbar\omega_M$ and $\hbar\omega_L$ with the correlation coefficients of >0.9995. The E_0 value of **ReB** evaluated by the simulation (15 800 cm^{-1}) was

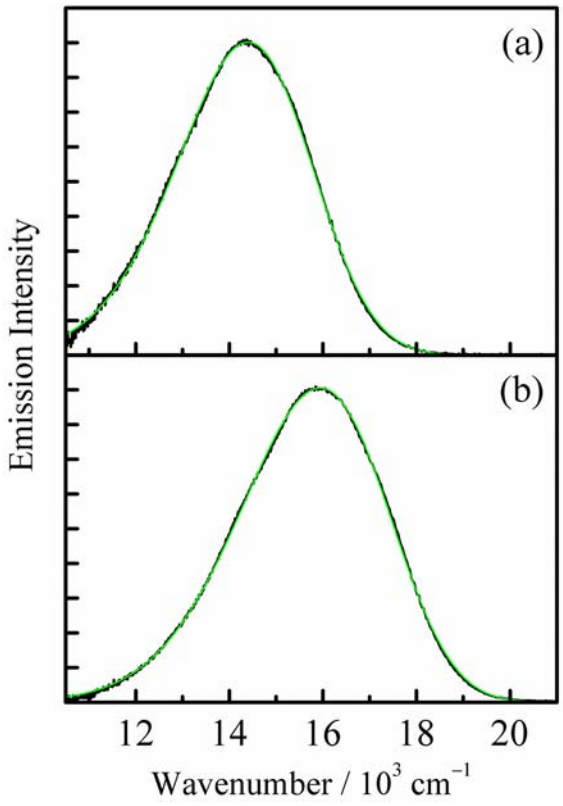

Figure 6. Corrected emission spectra in THF at 298 K (black) and the calculated fits (green) of **ReB** (a) and **RePhen** (b) based on eq 1 using the spectral parameters in Table 6.

Table 6. Spectral Fitting Parameters for ReB and RePhen in THF at 298 K

complex	E_0, cm^{-1}	$\tilde{\nu}_{1/2}$, cm^{-1}	$\hbar\omega_M$, cm^{-1}	S_M	$\hbar\omega_L$, cm^{-1}	S_L	r^a
ReB	15800	2430	1450	0.45	500	2.76	0.99954
RePhen	18000	2240	1450	0.69	500	3.82	0.99977

^{a}Correlation coefficient.

almost 2200 cm^{-1} smaller than that of **RePhen** (18 000 cm^{-1}), which agreed very well with the experimental observations, as described before. Furthermore, the $\hbar\omega_M$ and $\hbar\omega_L$ values of the complexes were evaluated to be 1450 and 500 cm^{-1}, respectively, which also agreed very well with the values reported for tricarbonyl rhenium(I) diimine complexes.[24b]

The medium- and low-frequency vibrational modes observed for the emission spectrum of a polydimine $d\pi^6$ transition metal complex are in general best characterized by the ring-breathing vibration in the diimine ligand and the stretching vibration between the metal ion and the ligating nitrogen atom, respectively. The results suggest that the DBDE group in **ReB** does not play an important role in determining the excited-state accepting frequencies of the complex. On the other hand, the Huang–Rhys factors observed for **ReB** ($S_M = 0.45$ and $S_L = 2.76$) were smaller than those of **RePhen** ($S_M = 0.69$ and $S_L = 3.82$). The results indicate that the vibrational displacements between the emitting ^{3}MLCT and ground states of **ReB** along the medium- and low-frequency mode coordinates are smaller than those of **RePhen** and, this could be one possible reason for the smaller k_r and k_{nr} values of **ReB** relative to the relevant value of **RePhen**: see Table 1. Furthermore, it was shown that the $\tilde{\nu}_{1/2}$

dx.doi.org/10.1021/ic3007469 | Inorg. Chem. 2012, 51, 7722–7732

Table 7. PET Emission Quenching of ReB and RePhen by Electron Donors in DMF at 298 K

				ReB			RePhen		
no.	quencher	$E_{1/2}(D^{+/0})$, V vs SCE	r_D, Å	ΔG_{ET}^0, eV	k_q, 10^8 $M^{-1}s^{-1}$	k'_q, 10^8 $M^{-1}s^{-1}$	ΔG_{ET}^0, eV	k_q, 10^8 $M^{-1}s^{-1}$	k'_q, 10^8 $M^{-1}s^{-1}$
1	carbazole	+1.16	4.7	+0.14	0.31	0.31	+0.097	1.1	1.1
2	aniline	+1.02	4.0	−0.0049	11	12	−0.052	7.0	7.7
3	diphenylamine	+0.89	4.8	−0.13	16	20	−0.17	13	15
4	*N*,*N*-dimethylaniline	+0.82	4.0	−0.21	33	57	−0.25	28	45
5	*o*-toluidine	+0.81	4.0	−0.21	15	18	−0.26	11	12
6	triethanolamine	+0.81	4.5	−0.12	0.89	0.90	−0.16	0.42	0.42
7	tri*n*-butylamine	+0.80	5.0	−0.22	4.8	5.2	−0.26	2.2	2.3
8	triethylamine	+0.80	4.2	−0.22	1.8	1.8	−0.27	0.91	0.92
9	1-*N*,*N*-dimethylaminonaphthalene	+0.79	4.5	−0.23	15	18	−0.28	12	15
10	phenothiazine	+0.61	4.8	−0.41	40	85.00	−0.45	42	100
11	*p*-phenylenediamine	+0.17	4.2	−0.85	39	78	−0.90	40	88

value of **ReB** (2430 cm^{-1}) was larger than that of **RePhen** (2240 cm^{-1}), which was induced clearly by the introduction of the DBDE group to the phen ligand in **ReB**. The results indicate the increase in the solvent interactions with the excited ^{3}MLCT state of **ReB** through the synergistic MLCT and π(aryl)-p(B) CT interactions.[7b,8]

Photoinduced Electron Transfer (PET) Quenching of the Excited States of the Complexes. To evaluate the photoredox ability of **ReB**, we studied PET emission quenching of **ReB** and **RePhen** by electron donors in DMF. The observed (k_q) and corrected PET emission quenching rate constant (k'_q) of the complexes determined for a series of quenchers are summarized in Table 7, together with the Gibbs free energy change for PET quenching (ΔG_{ET}^0) and the r_D values: see also the Experimental section. As a typical example, the emission decay profiles of **ReB** and **RePhen** in the absence and presence of triethanolamine (TEOA) as a quencher and the relevant Stern−Volmer plot are shown in Supporting Information: Figures S3 and S4, respectively. In the case of TEOA, the k'_q values of **ReB** and **RePhen** were determined to be 9.0×10^7 and 4.2×10^7 M^{-1} s^{-1}, respectively, indicating that the k'_q value of **ReB** was 2.1-times larger than that of **RePhen**. It is worth pointing out that the ΔG_{ET}^0 values of **ReB** and **RePhen** are −0.12 and −0.16 eV, respectively, demonstrating PET quenching of **ReB** is thermodynamically unfavorable compared with that of **RePhen**. For a given quencher, a similar trend to that of TEOA has been observed as confirmed by the data in Table 7, which should be clarified to demonstrate the characteristics of the PET reaction of **ReB**.

According to Scheme 2, the k'_q value can be given as in eq 8.

$$k'_q = k_{ET}\frac{k_d}{k_{-d}}\left(\frac{k'_{-d} + k_{BET}}{k'_{-d} + k_{BET} + k_{-ET}}\right) \quad (8)$$

For simplicity, we assume here that backward ET from the product ion pair to the encounter complex (k_{-ET}) is relatively slow compared with k'_{-d} and k_{BET} in the ΔG_{ET}^0 range studied (< +0.2 eV) and, thus, $(k'_{-d} + k_{BET}) \gg k_{-ET}$. If this is the case, eq 8 can be simplified as in eq 9.[32]

$$k'_q = k_{ET}\frac{k_d}{k_{-d}} = k_{ET}K_A \quad (9)$$

In eq 9, $K_A = k_d/k_{-d}$ is given by the Fuoss-Eigen equation,[33] $K_A = 4\pi N_A(r_A + r_D)^3/3000$ (N_A is the Avogadro's number), and it is considered to be almost constant irrespective of the nature of a quencher used. Furthermore, k_{ET} is given by eq 10:

$$k_{ET} = \nu_n \kappa \exp\left(-\frac{\Delta G_{ET}^{\ddagger}}{RT}\right) \quad (10)$$

where ν_n and κ are the vibrational frequency or an averaged frequency for a trapping vibration(s) and the single passage transmission coefficient for a PET event, respectively. In the classical regime by Rehm and Weller, the Gibbs activation energy of PET, $\Delta G_{ET}^{\ddagger}$, is given based on ΔG_{ET}^0 and the intrinsic Gibbs activation energy, $\Delta G_{ET}^{\ddagger}(0)$ ($\Delta G_{ET}^{\ddagger}$ at $\Delta G_{ET}^0 = 0$) as in eq 11.[34]

$$\Delta G_{ET}^{\ddagger} = \frac{\Delta G_{ET}^0}{2} + \sqrt{\left(\frac{\Delta G_{ET}^0}{2}\right)^2 + \{\Delta G_{ET}^{\ddagger}(0)\}^2} \quad (11)$$

As a result, eq 9 can be converted to eq 12.

$$RT \ln k'_q = RT \ln(K_A \nu_n \kappa) - \left[\frac{\Delta G_{ET}^0}{2} + \sqrt{\left(\frac{\Delta G_{ET}^0}{2}\right)^2 + \{\Delta G_{ET}^{\ddagger}(0)\}^2}\right] \quad (12)$$

The ΔG_{ET}^0 dependences of the k'_q values observed for **ReB** and **RePhen** are shown in Figure 7, and the data were fitted by eq 12 with $\Delta G_{ET}^{\ddagger}(0)$ being a fitting parameter. For the fittings, the data on the aliphatic amines (the data numbers 6, 7, and 8 in Table 7) were omitted since the data deviated obviously from the relationship between $RT\ln k'_q$ and ΔG_{ET}^0 for both the **ReB**/**RePhen**−aromatic amine systems. The small k'_q values observed for the aliphatic amines, as predicted from the relevant ΔG_{ET}^0

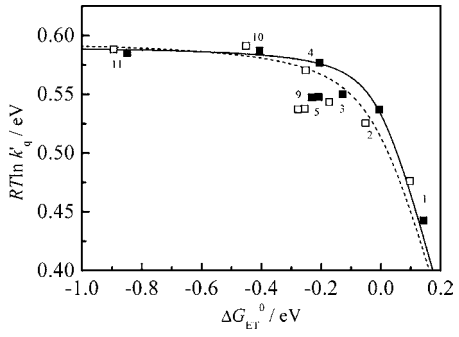

Figure 7. ΔG_{ET}^0 dependences of the k'_q values of **ReB** (■) and **RePhen** (□) in DMF. Data taken from Table 7 and the numbers correspond to those in Table 7. Solid and broken curves represent the theoretical fits for **ReB** and **RePhen**, respectively, based on eq 12.

dx.doi.org/10.1021/ic3007469 | Inorg. Chem. 2012, 51, 7722−7732

value, will be due to the relatively large structural change upon the ET event: large inner-sphere reorganization energy. In practice, similar behaviors of aliphatic amine quenchers have been reported for the PET reactions of chromium(III) and iridium(III) complexes by Scandola and co-workers.[35] By omitting the data on the aliphatic amines, the ΔG_{ET}^{0} dependences of $RT\ln k'_q$ were fitted very well by eq 12 for both complexes, and this gave $\Delta G_{ET}^{\ddagger}(0)$ to be 0.059 and 0.085 eV for **ReB** and **RePhen**, respectively. Thus, the present analysis demonstrates that the introduction of the DBDE group to the phen ligand gives rise to almost a 30% decrease in $\Delta G_{ET}^{\ddagger}(0)$, and this will be the main factor for the faster PET reaction observed for **ReB** compared with that of **RePhen** at given ΔG_{ET}^{0}.

According to the Marcus theory,[36] $\Delta G_{ET}^{\ddagger}$ is given by eq 13.

$$\Delta G_{ET}^{\ddagger} = \frac{(\lambda + \Delta G_{ET}^{0})^2}{4\lambda} \tag{13}$$

In eq 13, λ is the sum of the inner- (λ_i) and outer-sphere reorganization energies (λ_o) for ET, and $\Delta G_{ET}^{\ddagger}(0)$ corresponds to $\lambda/4$. Therefore, the smaller $\Delta G_{ET}^{\ddagger}(0)$ value of **ReB** compared with that of **RePhen** should be discussed in terms of λ_i and/or λ_o. In the limit of a dielectric continuum, λ_o for ET between noninterpenetrating spheres is given by eq 14,

$$\lambda_o = e^2\left(\frac{1}{2r_A} + \frac{1}{2r_D} - \frac{1}{d}\right)\left(\frac{1}{D_{opt}} - \frac{1}{D_s}\right) \tag{14}$$

where D_{opt} is the optical dielectric constant of a medium and is equal to the square of a refractive index. The λ_o value of **ReB** should be smaller than that of **RePhen**, since the value in general becomes smaller with increasing the radius of a molecule and, in practice, λ_o of **ReB** (r_A = 7.2 Å) and **RePhen** (r_A = 5.3 Å) in DMF for a given D (r_D = 4.4 Å) are calculated to be 0.65 and 0.70 eV, respectively. However, the λ_o value estimated based on the average molecular radius of **ReB** or **RePhen** (i.e., for given D and solvent) might be doubtful, since the two complexes are the structurally unsymmetrical compounds and, in particular, the ^{3}MLCT excited state of **ReB** will be more solvated compared with **RePhen** owing to the presence of the DBDE group in **ReB** as revealed by the $\tilde{\nu}_{1/2}$ value of the complex by the Franck–Condon analysis. On the other hand, our Franck–Condon analysis of the emission spectra of **ReB** and **RePhen** demonstrates that the structural change upon de-excitation (i.e., backward ET) of the ^{3}MLCT excited state of the complex is smaller for **ReB** compared with that of **RePhen**, suggesting the contribution of λ_i to $\Delta G_{ET}^{\ddagger}$. The λ_i value can be estimated as the sum of the energy for the structural changes of **ReB**/**RePhen** and D before and after an ET event. For a given D, we can consider the contribution of λ_i of the complex to the observed $\Delta G_{ET}^{\ddagger}(0)$, and the data by the Franck–Condon analysis of the emission spectrum mentioned above can provide information about λ_i through eq 15.

$$\lambda_{i,complex} = \sum_j S_j \hbar\omega_j \tag{15}$$

On the basis of the S_j and $\hbar\omega_j$ values estimated for the two complexes (see Table S1, Supporting Information), the $\lambda_{i,comlpex}$ values of **ReB** and **RePhen** are calculated to be 0.28 and 0.38 eV, respectively, indicating the difference in the value between the two complexes being 0.10 eV. Clearly, the value of $\Delta\Delta G_{ET}^{\ddagger}(0)$ theoretically evaluated by eq 13 ($\lambda/4$ = 0.025 eV) is comparable with the experimentally observed $\Delta\Delta G_{ET}^{\ddagger}(0)$ (0.026 eV). These discussions indicate that both λ_o and λ_i contribute moderately to $\Delta G_{ET}^{\ddagger}(0)$ of **ReB**, which is favorable for the PET reaction compared with that of **RePhen**. For PET/ET reactions of transition metal complexes, the contribution of λ_o to the reaction rate has been hitherto discussed frequently, while the discussion on the contribution of λ_i to $\Delta G_{ET}^{\ddagger}$ has not been necessarily straightforward. We convince that complementary works on both photophysical (i.e., Franck–Condon analysis) and PET (i.e., theoretical discussions) characteristics of a photosensitizer is of primary importance for development of an efficient photosensitizing system and a transition metal complex having an arylborane-appended ligand(s) showing intense visible absorption and long excited-state lifetime is a promising candidate for a future photoredox sensitizer.

CONCLUSIONS

The present results demonstrated that an introduction of an arylborane CT unit onto the aromatic diimine ligand in a tricarbonyl rhenium(I) complex influenced extraordinary the spectroscopic, photophysical, and photoredox properties of the complex compared with those of the complex without the arylborane substituent, **RePhen**. **ReB** showed low-energy absorption and phosphorescence (ν^{abs} = 23 800 cm^{-1} and E_0 = 15 800 cm^{-1} in THF) compared with those of **RePhen** (ν^{abs} = 26 000 cm^{-1} and E_0 = 18 000 cm^{-1} in THF). Despite the low-energy excited state, **ReB** showed relatively long-lived emission (τ^{em} = 900 ns in THF) owing to the increase in the energy barrier for the thermal deactivation process via a higher-energy nonemitting excited state (ΔE = 960 cm^{-1}).

Photoinduced electron transfer emission quenching experiments on **ReB** and **RePhen** by a series of electron donors and the analysis of the $RT\ln k'_q$ vs ΔG_{ET}^{0} plots demonstrated that the $\Delta G_{ET}^{\ddagger}(0)$ value observed for **ReB** was smaller than that of **RePhen**. This was explained by the small structural (λ_i) and solvation change (λ_o) upon ET of **ReB** compared with those of **RePhen**, which was reflected by the presence of the triarylborane group on the phen ligand in **ReB**. Although synthesis and spectroscopic properties of transition metal complexes having an arylborane substituent(s) have been hitherto reported,[12−17] this is the first demonstration of the photoredox characteristics of a transition metal complex with an arylborane-appended ligand. Since a transition metal complex having an arylborane-type ligand(s) in general show intense absorption in the visible region and a long excited-state lifetime,[10,13c,17] we convince that such a type of complexes play important roles in photoredox reactions and solar energy conversion systems.

ASSOCIATED CONTENT

Supporting Information

Synthesis/characterization of EDDB, Franck–Condon analysis for **ReB** and **RePhen** in DMF, temperature dependences of the emission decay profiles, and emission quenching data of the complexes by TEOA. This material is available free of charge via the Internet at http://pubs.acs.org.

AUTHOR INFORMATION

Corresponding Author

*E-mail: kitamura@sci.hokudai.ac.jp.

Present Address

[‖]Department of Chemistry, The University of North Carolina at Chapel Hill, Chapel Hill, North Carolina 27599, United States

Notes

The authors declare no competing financial interest.

■ ACKNOWLEDGMENTS

E.S. thanks the Global COE program of Hokkaido University (Catalysis as the Basis for Materials Innovation) for a research fellowship (2008−2010) and the F3 Project of MEXT, Japan (2010−present).

■ REFERENCES

(1) (a) Durham, B.; Caspar, J. V.; Nagle, J. K.; Meyer, T. J. *J. Am. Chem. Soc.* **1982**, *104*, 4803. (b) Kalyanasundaram, K. *Coord. Chem. Rev.* **1982**, *46*, 159. (c) Caspar, J. V.; Meyer, T. J. *J. Am. Chem. Soc.* **1983**, *105*, 5583. (d) Kitamura, N.; Kawanishi, Y.; Tazuke, S. *Chem. Phys. Lett.* **1983**, *97*, 103. (e) Kawanishi, Y.; Kitamura, N.; Tazuke, S. *Inorg. Chem.* **1989**, *28*, 2968. (f) Fleming, C. N.; Maxwell, K. A.; DeSimone, J. M.; Meyer, T. J.; Papanikolas, J. M. *J. Am. Chem. Soc.* **2001**, *123*, 10336.

(2) (a) Sacksteder, L.; Zipp, A. P.; Brown, E. A.; Streich, J.; Demas, J. N.; DeGraff, B. A. *Inorg. Chem.* **1990**, *29*, 4335. (b) Wallace, L.; Rillema, D. P. *Inorg. Chem.* **1993**, *32*, 3836. (c) Ferraudi, G.; Feliz, M.; Wolcan, E.; Hsu, I.; Moya, S. A.; Guerrero, J. *J. Phys. Chem.* **1995**, *99*, 4929. (d) Wallace, L.; Jackman, D. C.; Rillema, D. P.; Merkert, J. W. *Inorg. Chem.* **1995**, *34*, 5210. (e) Shaver, R. J.; Perkovic, M. W.; Rillema, D. P.; Woods, C. *Inorg. Chem.* **1995**, *34*, 5446. (f) Itokazu, M. K.; Polo, A. S.; de Faria, D. L. A.; Bignozzi, C. A.; Iha, N. Y. M. *Inorg. Chim. Acta* **2001**, *313*, 149. (g) Striplin, D. R.; Crosby, G. A. *Coord. Chem. Rev.* **2001**, *211*, 163. (h) Koike, K.; Okoshi, N.; Hori, H.; Takeuchi, K.; Ishitani, O.; Tsubaki, H.; Clark, I. P.; George, M. W.; Johnson, F. P. A.; Turner, J. J. *J. Am. Chem. Soc.* **2002**, *124*, 11448. (i) Sun, S.-S.; Lees, A. J. *Coord. Chem. Rev.* **2002**, *230*, 171. (j) Rajendran, T.; Manimaran, B.; Liao, R.-T.; Lin, R.-J.; Thanasekaran, P.; Lee, G.-H.; Peng, S.-M.; Liu, Y.-H.; Chang, I.-J.; Rajagopal, S.; Lu, K.-L. *Inorg. Chem.* **2003**, *42*, 6388. (k) Ranjan, S.; Lin, S.-Y.; Hwang, K.-C.; Chi, Y.; Ching, W.-L.; Liu, C.-S.; Tao, Y.-T.; Chien, C.-H.; Peng, S.-M.; Lee, G.-H. *Inorg. Chem.* **2003**, *42*, 1248. (l) Wenger, O. S.; Henling, L. M.; Day, M. W.; Winkler, J. R.; Gray, H. B. *Inorg. Chem.* **2004**, *43*, 2043. (m) Lo, K. K.-W.; Tsang, K. H.-K.; Hui, W.-K.; Zhu, N. *Inorg. Chem.* **2005**, *44*, 6100. (n) Thanasekaran, P.; Liao, R.-T.; Liu, Y.-H.; Rajendran, T.; Rajagopal, S.; Lu, K.-L. *Coord. Chem. Rev.* **2005**, *249*, 1085. (o) Villegas, J. M.; Stoyanov, S. R.; Huang, W.; Rillema, D. P. *Inorg. Chem.* **2005**, *44*, 2297. (p) Kirgan, R.; Simpson, M.; Moore, C.; Day, J.; Bui, L.; Tanner, C.; Rillema, D. P. *Inorg. Chem.* **2007**, *46*, 6464. (q) Sato, S.; Sekine, A.; Ohashi, Y.; Ishitani, O.; Blanco-Rodríguez, A. M.; Vlček, A.; Unno, T.; Koike, K. *Inorg. Chem.* **2007**, *46*, 3531. (r) Coleman, A.; Brennan, C.; Vos, J. G.; Pryce, M. T. *Coord. Chem. Rev.* **2008**, *252*, 2585. (s) Yamamoto, Y.; Sawa, S.; Funada, Y.; Morimoto, T.; Falkenström, M.; Miyasaka, H.; Shishido, S.; Ozeki, T.; Koike, K.; Ishitani, O. *J. Am. Chem. Soc.* **2008**, *130*, 14659. (t) Ko, C.-C.; Lo, L. T.-L.; Ng, C.-O.; Yiu, S.-M. *Chem.−Eur. J* **2010**, *16*, 13773. (u) Patrocinio, A. O. T.; Brennaman, M. K.; Meyer, T. J.; Murakami Iha, N. Y. *J. Phys. Chem. A* **2010**, *114*, 12129. (v) Machura, B.; Wolff, M.; Jaworska, M.; Lodowski, P.; Benoist, E.; Carrayon, C.; Saffon, N.; Kruszynski, R.; Mazurak, Z. *J. Organomet. Chem.* **2011**, *696*, 3068.

(3) (a) Hawecker, J.; Lehn, J.-M.; Ziessel, R. *J. Chem. Soc., Chem. Commun.* **1983**, 536. (b) Hawecker, J.; Lehn, J.-M.; Ziessel, R. *Helv. Chim. Acta* **1986**, *69*, 1990. (c) Ziessel, R.; Hawecker, J.; Lehn, J.-M. *Helv. Chim. Acta* **1986**, *69*, 1065. (d) Hori, H.; Johnson, F. P. A.; Koike, K.; Ishitani, O.; Ibusuki, T. *J. Photochem. Photobiol. A: Chem* **1996**, *96*, 171. (e) Hori, H.; Koike, K.; Ishizuka, M.; Takeuchi, K.; Ibusuki, T.; Ishitani, O. *J. Organomet. Chem.* **1997**, *530*, 169. (f) Gholamkhass, B.; Mametsuka, H.; Koike, K.; Tanabe, T.; Furue, M.; Ishitani, O. *Inorg. Chem.* **2005**, *44*, 2326. (g) Tsubaki, H.; Sekine, A.; Ohashi, Y.; Koike, K.; Takeda, H.; Ishitani, O. *J. Am. Chem. Soc.* **2005**, *127*, 15544. (h) Takeda, H.; Koike, K.; Inoue, H.; Ishitani, O. *J. Am. Chem. Soc.* **2008**, *130*, 2023. (i) Koike, K.; Naito, S.; Sato, S.; Tamaki, Y.; Ishitani, O. *J. Photochem. Photobiol. A: Chem.* **2009**, *207*, 109. (j) Takeda, H.; Ishitani, O. *Coord. Chem. Rev.* **2010**, *254*, 346. (k) Agarwal, J.; Johnson, R. P.; Li, G. *J. Phys. Chem. A* **2011**, *115*, 2877.

(4) (a) Lees, A. J. *Chem. Rev.* **1987**, *87*, 711. (b) Kurz, P.; Probst, B.; Spingler, B.; Alberto, R. *Eur. J. Inorg. Chem.* **2006**, *2006*, 2966.

(5) (a) Caspar, J. V.; Meyer, T. J. *J. Phys. Chem.* **1983**, *87*, 952. (b) Chen, P. Y.; Duesing, R.; Graff, D. K.; Meyer, T. J. *J. Phys. Chem.* **1991**, *95*, 5850. (c) Carballo, R.; Castiñeiras, A.; García-Fontán, S.; Losada-González, P.; Abram, U.; Vázquez-López, E. M. *Polyhedron* **2001**, *20*, 2371. (d) Claude, J. P.; Omberg, K. M.; Williams, D. S.; Meyer, T. J. *J. Phys. Chem. A* **2002**, *106*, 7795.

(6) Brown, H. C.; Dodson, V. H. *J. Am. Chem. Soc.* **1957**, *79*, 2302.

(7) (a) Yamaguchi, S.; Akiyama, S.; Tamao, K. *J. Am. Chem. Soc.* **2000**, *122*, 6335. (b) Kitamura, N.; Sakuda, E. *J. Phys. Chem. A* **2005**, *109*, 7429. (c) Kitamura, N.; Sakuda, E.; Yoshizawa, T.; Iimori, T.; Ohta, N. *J. Phys. Chem. A* **2005**, *109*, 7435. (d) Kitamura, N.; Sakuda, E.; Ando, Y. *Chem. Lett.* **2009**, *38*, 938.

(8) Sakuda, E.; Ando, Y.; Ito, A.; Kitamura, N. *J. Phys. Chem. A* **2010**, *114*, 9144.

(9) Sakuda, E.; Tsuge, K.; Sasaki, Y.; Kitamura, N. *J. Phys. Chem. B* **2005**, *109*, 22326.

(10) Sakuda, E.; Funahashi, A.; Kitamura, N. *Inorg. Chem.* **2006**, *45*, 10670.

(11) Aldridge, T. K.; Stacy, E. M.; McMillin, D. R. *Inorg. Chem.* **1994**, *33*, 722.

(12) (a) Sun, Y.; Ross, N.; Zhao, S.-B.; Huszarik, K.; Jia, W.-L.; Wang, R.-Y.; Macartney, D.; Wang, S. *J. Am. Chem. Soc.* **2007**, *129*, 7510. (b) Zhao, S.-B.; McCormick, T.; Wang, S. *Inorg. Chem.* **2007**, *46*, 10965. (c) Hudson, Z. M.; Zhao, S.-B.; Wang, R.-Y.; Wang, S. *Chem.−Eur. J.* **2009**, *15*, 6131. (d) Rao, Y.-L.; Wang, S. *Inorg. Chem.* **2009**, *48*, 7698. (e) Sun, Y.; Wang, S. *Inorg. Chem.* **2009**, *48*, 3755. (f) Hudson, Z. M.; Sun, C.; Helander, M. G.; Amarne, H.; Lu, Z.-H.; Wang, S. *Adv. Funct. Mater.* **2010**, *20*, 3426. (g) Sun, Y.; Wang, S. *Inorg. Chem.* **2010**, *49*, 4394. (h) Hudson, Z. M.; Helander, M. G.; Lu, Z.-H.; Wang, S. *Chem. Commun.* **2011**, *47*, 755. (i) Hudson, Z. M.; Sun, C.; Harris, K. J.; Lucier, B. E. G.; Schurko, R. W.; Wang, S. *Inorg. Chem.* **2011**, *50*, 3447. (j) Hudson, Z. M.; Wang, S. *Organometallics* **2011**, *30*, 4695.

(13) (a) You, Y.; Park, S. Y. *Adv. Mater.* **2008**, *20*, 3820. (b) Zhou, G.; Ho, C.-L.; Wong, W.-Y.; Wang, Q.; Ma, D.; Wang, L.; Lin, Z.; Marder, T. B.; Beeby, A. *Adv. Funct. Mater.* **2008**, *18*, 499. (c) Ito, A.; Hiokawa, T.; Sakuda, E.; Kitamura, N. *Chem. Lett.* **2011**, *40*, 34. (d) Vadavi, R. S.; Kim, H.; Lee, K. M.; Kim, T.; Lee, J.; Lee, Y. S.; Lee, M. H. *Organometallics* **2011**, *31*, 31.

(14) (a) Wade, C. R.; Gabbaï, F. P. *Inorg. Chem.* **2009**, *49*, 714. (b) Sun, Y.; Hudson, Z. M.; Rao, Y.; Wang, S. *Inorg. Chem.* **2011**, *50*, 3373.

(15) (a) Lam, S.-T.; Zhu, N.; Yam, V. W.-W. *Inorg. Chem.* **2009**, *48*, 9664. (b) Wang, J.; Bai, F.-Q.; Xia, B.-H.; Chen, J.; Zhang, H.-X. *J. Organomet. Chem.* **2011**, *696*, 2943.

(16) Hudson, Z. M.; Wang, S. *Dalton Trans.* **2011**, *40*, 7805.

(17) Sakuda, E.; Ando, Y.; Ito, A.; Kitamura, N. *Inorg. Chem.* **2011**, *50*, 1603.

(18) Sakuda, E.; Tanaka, M.; Ito, A.; Kitamura, N. *RSC Adv.* **2012**, *2*, 1296.

(19) Yamaguchi, S.; Shirasaka, T.; Tamao, K. *Org. Lett.* **2000**, *2*, 4129.

(20) (a) Poe, D. P.; Eppen, A. D.; Whoolery, S. P. *Talanta* **1980**, *27*, 368. (b) Bijeire, L.; Legentil, L.; Bastide, J.; Darro, F.; Rochart, C.; Delfourne, E. *Eur. J. Org. Chem.* **2004**, *2004*, 1891.

(21) Perrin, D. D.; Armarego, W. L. F.; Perrin, D. R. *Purification of Laboratory Chemicals*; Pargamon Press: New York, 1980.

(22) (a) Suzuki, K.; Kobayashi, A.; Kaneko, S.; Takehira, K.; Yoshihara, T.; Ishida, H.; Shiina, Y.; Oishi, S.; Tobita, S. *Phys. Chem. Chem. Phys.* **2009**, *11*, 9850. (b) Ishida, H.; Tobita, S.; Hasegawa, Y.; Katoh, R.; Nozaki, K. *Coord. Chem. Rev.* **2010**, *254*, 2449.

(23) Frisch, M. J.; Trucks, G. W.; Schlegel, H. B.; Scuseria, G. E.; Robb, M. A.; Cheeseman, J. R.; Scalmani, G.; Barone, V.; Mennucci, B.; Petersson, G. A.; Nakatsuji, H.; Caricato, M.; Li, X.; Hratchian, H. P.; Izmaylov, A. F.; Bloino, J.; Zheng, G.; Sonnenberg, J. L.; Hada, M.; Ehara, M.; Toyota, K.; Fukuda, R.; Hasegawa, J.; Ishida, M.; Nakajima, T.; Honda, Y.; Kitao, O.; Nakai, H.; Vreven, T.; J. A. Montgomery, J.; Peralta, J. E.; Ogliaro, F.; Bearpark, M.; Heyd, J. J.; Brothers, E.; Kudin, K. N.; Staroverov, V. N.; Kobayashi, R.; Normand, J.; Raghavachari, K.; Rendell, A.; Burant, J. C.; Iyengar, S. S.; Tomasi, J.; Cossi, M.; Rega, N.;

Millam, J. M.; Klene, M.; Knox, J. E.; Cross, J. B.; Bakken, V.; Adamo, C.; Jaramillo, J.; Gomperts, R.; Stratmann, R. E.; Yazyev, O.; Austin, A. J.; Cammi, R.; Pomelli, C.; Ochterski, J. W.; Martin, R. L.; Morokuma, K.; Zakrzewski, V. G.; Voth, G. A.; Salvador, P.; Dannenberg, J. J.; Dapprich, S.; Daniels, A. D.; Farkas, O.; Foresman, J. B.; Ortiz, J. V.; Cioslowski, J.; Fox, D. J. *Gaussian 09*, Revision A.1; Gaussian, Inc.: Wallingford, CT, 2009.

(24) (a) Allen, G. H.; White, R. P.; Rillema, D. P.; Meyer, T. J. *J. Am. Chem. Soc.* **1984**, *106*, 2613. (b) Caspar, J. V.; Westmoreland, T. D.; Allen, G. H.; Bradley, P. G.; Meyer, T. J.; Woodruff, W. H. *J. Am. Chem. Soc.* **1984**, *106*, 3492. (c) Kim, H.-B.; Kitamura, N.; Tazuke, S. *J. Phys. Chem.* **1990**, *94*, 7401. (d) Nozaki, K.; Takamori, K.; Nakatsugawa, Y.; Ohno, T. *Inorg. Chem.* **2006**, *45*, 6161.

(25) Huang, K.; Rhys, A. *Proc. R. Soc. London, Ser. A* **1950**, *204*, 406.

(26) (a) Parker, C. A.; Rees, W. T. *Analyst* **1960**, *85*, 587. (b) Valeur, B. *Molecular Fluorescence: Principles and Applications*; Wiley-VCH: Weinheim: New York, 2006.

(27) Fylstra, D.; Lasdon, L.; Watson, J.; Waren, A. *Interfaces* **1998**, *28*, 29.

(28) von Smoluchowski, M. *Z. Phys. Chem., Stoechiom. Verwandtschaftsl.* **1917**, *92*, 129.

(29) Kitamura, N.; Kim, H.-B.; Okano, S.; Tazuke, S. *J. Phys. Chem.* **1989**, *93*, 5750.

(30) (a) Caspar, J. V.; Meyer, T. J. *Inorg. Chem.* **1983**, *22*, 2444. (b) Kober, E. M.; Caspar, J. V.; Lumpkin, R. S.; Meyer, T. J. *J. Phys. Chem.* **1986**, *90*, 3722. (c) Chen, P.; Meyer, T. J. *Chem. Rev.* **1998**, *98*, 1439.

(31) Forster, L. S. *Coord. Chem. Rev.* **2002**, *227*, 59.

(32) Meyer, T. J. *Prog. Inorg. Chem.* **1983**, *30*, 389.

(33) (a) Eigen, M. *Z. Phys. Chem. (Frankfurt am Main)* **1954**, *1*, 176. (b) Fuoss, R. M. *J. Am. Chem. Soc.* **1958**, *80*, 5059.

(34) Rehm, D.; Weller, A. *Ber. Bunsen−Ges. Phys. Chem* **1969**, *73*, 834.

(35) Ballardini, R.; Varani, G.; Indelli, M. T.; Scandola, F.; Balzani, V. *J. Am. Chem. Soc.* **1978**, *100*, 7219.

(36) (a) Marcus, R. A. *J. Chem. Phys.* **1956**, *24*, 966. (b) Marcus, R. A. *J. Chem. Phys.* **1956**, *24*, 979. (c) Marcus, R. A. *Annu. Rev. Phys. Chem.* **1964**, *15*, 155.

■ NOTE ADDED AFTER ASAP PUBLICATION

Due to a production error, this paper was published on the Web on June 28, 2012, with a minor text error. The corrected version was reposted on June 29, 2012.